



AFRL-AFOSR-VA-TR-2019-0200

---

**Tailoring Piezoiimpedance Surface and Configurations of Carbon Nanotube Yarn Sensors for Integrated Damage Detection in Composite Materials**

**Kalayu Belay**  
**Florida Agricultural and Mechanical University Tallahassee**

---

**12/14/2018**  
**Final Report**

**DISTRIBUTION A: Distribution approved for public release.**

**Air Force Research Laboratory**  
**AF Office Of Scientific Research (AFOSR)/ RTA1**  
**Arlington, Virginia 22203**  
**Air Force Materiel Command**

DISTRIBUTION A: Distribution approved for public release.

<b>REPORT DOCUMENTATION PAGE</b>			<i>Form Approved</i> OMB No. 0704-0188	
<p>The public reporting burden for this collection of information is estimated to average 1 hour per response, including the time for reviewing instructions, searching existing data sources, gathering and maintaining the data needed, and completing and reviewing the collection of information. Send comments regarding this burden estimate or any other aspect of this collection of information, including suggestions for reducing the burden, to Department of Defense, Executive Services, Directorate (0704-0188). Respondents should be aware that notwithstanding any other provision of law, no person shall be subject to any penalty for failing to comply with a collection of information if it does not display a currently valid OMB control number.</p> <p><b>PLEASE DO NOT RETURN YOUR FORM TO THE ABOVE ORGANIZATION.</b></p>				
<b>1. REPORT DATE (DD-MM-YYYY)</b> 23-07-2019		<b>2. REPORT TYPE</b> Final Performance		<b>3. DATES COVERED (From - To)</b> 15 Jun 2015 to 14 Sep 2018
<b>4. TITLE AND SUBTITLE</b> Tailoring Piezoimpedance Surface and Configurations of Carbon Nanotube Yarn Sensors for Integrated Damage Detection in Composite Materials			<b>5a. CONTRACT NUMBER</b>	
			<b>5b. GRANT NUMBER</b> FA9550-15-1-0177	
			<b>5c. PROGRAM ELEMENT NUMBER</b> 61102F	
<b>6. AUTHOR(S)</b> Kalayu Belay, Jandro Abot			<b>5d. PROJECT NUMBER</b>	
			<b>5e. TASK NUMBER</b>	
			<b>5f. WORK UNIT NUMBER</b>	
<b>7. PERFORMING ORGANIZATION NAME(S) AND ADDRESS(ES)</b> Florida Agricultural and Mechanical University Tallahassee 1500 Wahnish Way Tallahassee, FL 32307-3100 US			<b>8. PERFORMING ORGANIZATION REPORT NUMBER</b>	
<b>9. SPONSORING/MONITORING AGENCY NAME(S) AND ADDRESS(ES)</b> AF Office of Scientific Research 875 N. Randolph St. Room 3112 Arlington, VA 22203			<b>10. SPONSOR/MONITOR'S ACRONYM(S)</b> AFRL/AFOSR RTA I	
			<b>11. SPONSOR/MONITOR'S REPORT NUMBER(S)</b> AFRL-AFOSR-VA-TR-2019-0200	
<b>12. DISTRIBUTION/AVAILABILITY STATEMENT</b> A DISTRIBUTION UNLIMITED: PB Public Release				
<b>13. SUPPLEMENTARY NOTES</b>				
<b>14. ABSTRACT</b> Laminated polymeric composites are excellent materials due to their high specific stiffness and strength as well as manufacturing tailorability. Consequently, they are being increasingly used in aerospace applications including various structural components. Existing nondestructive evaluation and structural health monitoring techniques can monitor their condition and integrity, but they are still unable to assess the condition of composite structures in a simple way and in realtime. This project is about investigating the piezoresistive response of carbon nanotube yarns towards their use as sensors in integrated structural health monitoring and developing the know-how to implement damage detection and strain measurement in polymers and composites, and sensing in other applications like temperature and torque measurement. The progress in determining the piezoresistive response of the carbon nanotube yarns has been significant and a more detailed understanding is now available.				
<b>15. SUBJECT TERMS</b> carbon nanotube, damage detection, composite, piezoimpedance				
<b>16. SECURITY CLASSIFICATION OF:</b>			<b>17. LIMITATION OF ABSTRACT</b>  UU	<b>18. NUMBER OF PAGES</b>
<b>a. REPORT</b>  Unclassified	<b>b. ABSTRACT</b>  Unclassified	<b>c. THIS PAGE</b>  Unclassified		
			<b>19a. NAME OF RESPONSIBLE PERSON</b> TILEY, JAIMIE	
			<b>19b. TELEPHONE NUMBER (Include area code)</b> 703-588-8316	

Standard Form 298 (Rev. 8/98)  
Prescribed by ANSI Std. Z39.18

DISTRIBUTION A: Distribution approved for public release.

**Annual and Final Report Annual report covering June 15, 2015 – September 14,  
2018**

**On the AFOSR-Funded Project**

**Air Force grant Award No. FA9550-15-1-0177**

**Tailoring Piezoimpedance, Surface and Configurations of Carbon Nanotube Yarn  
Sensors for Integrated Damage Detection in Composite Materials**

PI: Dr. Kalayu Belay  
111 Jones Hall  
Department of Physics  
Florida A&M University  
Tallahassee, FL 32307  
Phone: 850-599-3815  
Fax: 850-599-3577  
E-mail: [kalayu.belay@fam.u.edu](mailto:kalayu.belay@fam.u.edu)

Co-PI: Dr. Jandro L. Abot,  
Associate Professor  
Department of Mechanical Engineering  
Materials Science and Engineering Program  
The Catholic University of America  
E-mail: [abot@catholic.edu](mailto:abot@catholic.edu)  
Office: G21 Pangborn Hall  
Mail: 620 Michigan Ave. NE  
Washington, DC 20064  
Telephone: (202) 319-4382  
Facsimile: (202) 319-5173

Program Officer: Dr. Jaimie Tiley  
Multiscale Structural Mechanics and Prognosis Portfolio  
Low Density Materials Portfolio  
Air Force Office of Scientific Research AFOSR/RTA  
875 N. Randolph Street  
Arlington VA 22203-1768  
E-mail: [jaimie.tiley@us.af.mil](mailto:jaimie.tiley@us.af.mil)  
(w) 703-588-8316

## **Abstract**

Laminated polymeric composites are excellent materials due to their high specific stiffness and strength as well as manufacturing tailorability. Consequently, they are being increasingly used in aerospace applications including various structural components. Existing nondestructive evaluation and structural health monitoring techniques can monitor their condition and integrity, but they are still unable to assess the condition of composite structures in a simple way and in real-time. This project is about investigating the piezoresistive response of carbon nanotube yarns towards their use as sensors in integrated structural health monitoring and developing the know-how to implement damage detection and strain measurement in polymers and composites, and sensing in other applications like temperature and torque measurement. The progress in determining the piezoresistive response of the carbon nanotube yarns has been significant and a more detailed understanding is now available. Parametric experiments were conducted to include the effect of quasi-static strain rate, strain level, twist, impregnation and yarn geometry on their piezoresistivity. Strain rates affect the failure mechanisms and electromechanical properties of CNT yarns; high strain rates exhibit increased tensile strength and a positive piezoresistivity while low strain rates favor a higher strain-to-failure and a negative piezoresistivity. The sensitivity of the CNT yarn remains relatively unchanged with varying strain rates, but strongly dependent on the strain level and yarn geometry. The linearity needed for a robust sensor is favored at higher strain rates. Due to the interplay of inter-tube slippage and structural reformation with twist, there is an optimal twist level to achieve desired properties. Low-twist CNT yarns (twist angle of 10-25°) exhibit a lower breaking strength, lower strain-to-failure but higher rigidity compared to medium- (25-35°) and high-twist CNT yarns (>35°). The piezoresistive response of the studied CNT yarns was found to be highest at medium twist. CNT yarn strain sensors made by embedding the yarn completely in a flexible substrate achieved ultimate strains of up to 50 % and gage factors greater than 1000; i.e., one and three order/s of magnitude greater than the bare yarn, respectively.

This study demonstrates also the capability of CNT yarn sensors in strain sensing and damage detection, with potential applications as torques sensors, flexible strain gauges, wearable sensors and in health monitoring of composites. Strain measurement on the surface using foil gauges consisting of carbon nanotube yarns is also being investigated. The first set of prototypes was fabricated and calibrated in our laboratory facilities. The localized detection of delamination and damage in laminated composites in real time is also being achieved using a network of integrated carbon nanotube yarns and validated through integrated fiber optic sensors and x-ray microtomography. Preliminary results indicate that they both confirm the results obtained with the CNT yarn sensors.

## **Objectives**

The research objective of the project is to tailor the surface and piezoimpedance response of carbon nanotube yarns so that they could be used as integrated sensors in polymers and composite materials for structural health monitoring and other sensing applications. These sensors are integrated in composite structures and are sensitive to local strain changes and various composite damage modes and thus render the structure with self-sensing capabilities without altering the integrity of the structure and without adding significant weight.

## **Status of Effort**

Progress has been made in all areas of the project and the scope of the project was also expanded to include new, related and relevant studies. The details of the results obtained this year are presented next.

## **New Results**

The new results obtained this year are categorized among six different areas: the characterization of the CNT yarns including mechanical, electrical and piezoresistive responses; the damage detection in composite materials using CNT yarns; the strain measurement using CNT yarns; the temperature measurement using CNT yarns; torque measurement using CNT yarns; and wearable sensors using CNT yarns.

### Characterization of CNT Yarns

Among the new studies this year are the effect of twist on the mechanical, electrical and piezoresistive properties. Figure 1 shows the different types of CNT yarns used in the study. The highlights of the results are presented next.

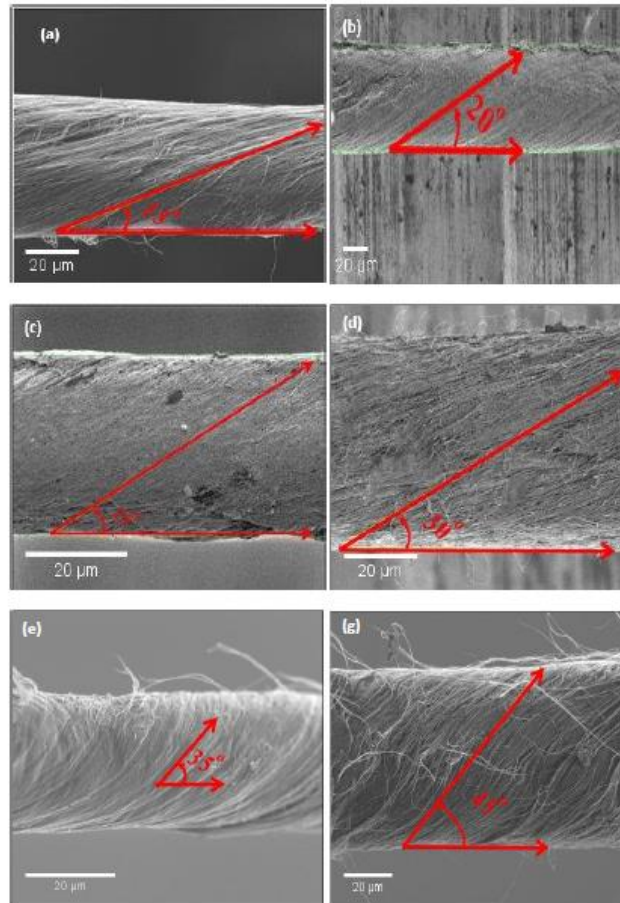


**Figure 1.** Micrographs of the CNT yarns studied indicating the twist angles: (a) 15°; (b) 20°; (c) 25°; (d) 30°; (e) 35°; (f) 45°.

*Mechanical Properties: Twist-Strength [8, 30].* Figure 2 shows strength-twist relationship of CNT yarn and conventional yarns. Fig. 2a and Figure 2b show a similarity in pattern from low tenacity at low twist to high tenacity at the medium twist range before showing a decline in tenacity at further twist ranges. This trend could be explained by the numerous parameters in the structure of spun yarns that affect their strength, from coherency to obliquity. Such enormous variability in the structure of spun yarns makes it very difficult to make uniform the different parameters affecting yarn's strength. To understand the role of both coherency and obliquity on the tenacity of CNT yarn, it is important to discuss the role they play in twist formation. CNT ribbons drawn from an array have very low mechanical strength and thus, are twisted to form stronger yarns. The lack of strength observed in the (untwisted) ribbons is associated with the parallel orientation of the fiber bundles to the yarn axis. Untwisted yarns have low interfacial contact between the fiber bundles and hence, low-to-zero binding force. Such yarns will exhibit similar characteristics to parallel fibers that fail under sheer amount of slippage. Under the action of twist, the induced lateral force increases the interfacial contact leading to increased inter-tube friction. As the twist level increases, the inter-tube friction increases, so does the yarn's packing density. The increased packing density means that more fiber bundles are

connected in bonds along the length of the yarn, increasing their resistance to slippage through friction. Further increase in twist will continue to bind the fiber bundles until they start to interlock.

Fiber locking occurs by the transfer of tensile stress to transverse stress during tensile deformation due to high twist action. As stress is continuously built up in the yarn under tension, the fiber locking effect becomes dominant limiting any inter-fiber bundle shear motion or slippage, and consequently, improving the strength of the yarn. During tensile loading of the yarn, the apparent stress-strain behavior will generally have a short linear region characterized by slippage of the fiber bundles followed by nonlinearity with considerable extension while the fiber bundles continue to slip, and finally failure occurs. Hearle's equation can be used to quantify the twist-strength effect in yarn structures:

$$\frac{\sigma_y}{\sigma_f} = \cos^2 \alpha (1 - k \csc \alpha) \quad (1)$$

where,  $\frac{\sigma_y}{\sigma_f}$  is the ratio of the yarn strength to the fiber bundle strength,  $\alpha$  is the helix angle that the constituent fiber/bundles make with the yarn axis. The term  $(1 - k \csc \alpha)$  represent the fiber locking, where  $k$  is a constant given by:

$$k = \left(\frac{dQ}{\mu}\right)^{\frac{1}{2}} / 3L \quad (2)$$

where  $d$  is the diameter of the fiber,  $Q$  is the fiber migration length,  $\mu$  is the coefficient of friction, and  $L$  is the length of the fiber. From Eqs. (1,2), increasing the coefficient of friction and length of the fiber and decreasing the diameter and the migration length will result in an increase in the strength of the yarn. However, there is a level of twist associated with the maximum strength of the yarn. The tensile strength of CNT yarns increases as twist increases to an optimum twist level, beyond which the strength of the yarn starts to decrease. Beyond this optimum, fiber bundles are oriented far away from the yarn's axis that the contribution of the fiber bundles strength to the yarn's strength becomes ineffective. This will reduce the overall strength of the yarn. The two effects are contrasting. The increase in strength with twist is associated with increase in fiber cohesion under twist while the decrease in strength with twist is associated with fiber obliquity under high twist reducing the contribution of the fiber strength to that of the yarn. Below this optimum, the yarn will fail through fiber slippage by the failure of the bundles while above the optimum; the yarn will fail by yarn fracture (Figure 2a).

The CNT yarn of varying twist showed an optimum strength at 30° twist as seen in Figure 2a. Miao observed that the tenacity of a flyer-spun twisted yarn reached its peak at about 15,000 T/m and then decreased slowly as twist level was further increased, as shown by the trend curve in Figure 2c. The optimum strength close to intermediate twist angle seem to agree with that of conventional yarn as seen in Figure 2b. The key difference however, is that the optimum strength of the CNT yarn is achieved at about 30° twist angle while that of textile yarns is closer to 50° twist angle. Stronger fibers can produce yarns with optimum strength at lower twist angles. For example, polyester fibers (breaking strength of 35-60 cN/tex) have optimum yarn strength at lower twist level compared to cotton fiber (breaking strength of 15-40 cN/tex). The difference could also be related to the difference in mechanisms of the inter-fiber bundle association, degree of alignment and the interfacial surface energy of CNTs. Whereas a cotton yarn has between 30-100 individual fibers in a yarn cross-section and a synthetic fiber yarn up to 100 fibers, a 10 μm-CNT yarn

is estimated to comprise of between 51,000 and 115,000 bundles in its cross-section. This is over three orders of magnitude difference in the fibrils in the cross-section of CNT yarns to that of conventional textile yarns. The van der Waals interconnections between CNTs plays a key role in the load transfer mechanism in a CNT yarn. Typically, in conventional yarns, the inter-fiber shear forces dictate the strength. CNT yarns, mostly dry spun yarns depend on this weak van der Waals connections between the CNTs to form and maintain a yarn structure. The CNT yarns used in this study were produced from highly aligned CNT arrays. The high alignment of CNT arrays is ensured by controlling the length or height of the array through growth time for example. The tenacity of the yarn would be lowest at the lowest twist level as observed in Figure 3. The tenacity of the CNT yarn with medium twist was significantly higher than that of the high twist. This is agreement to conventional understanding of twist-strength relationship in textile yarns. It is also important in the selection of twist level based on applications.

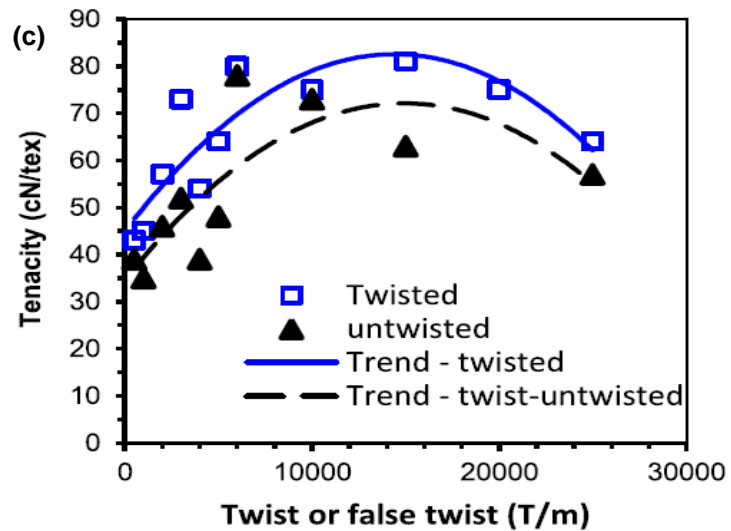
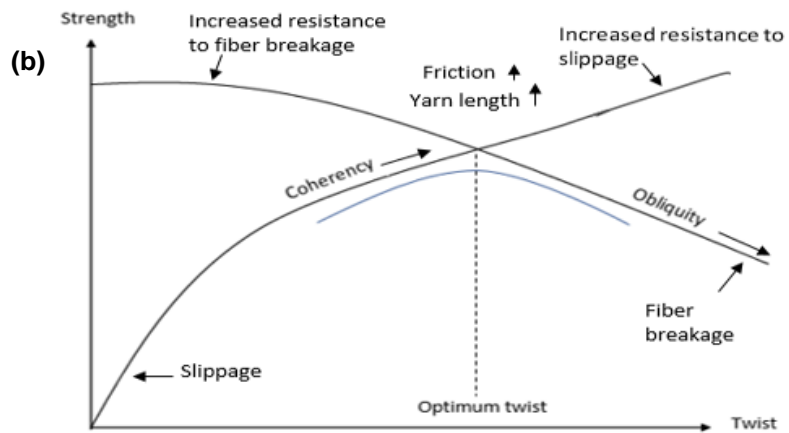
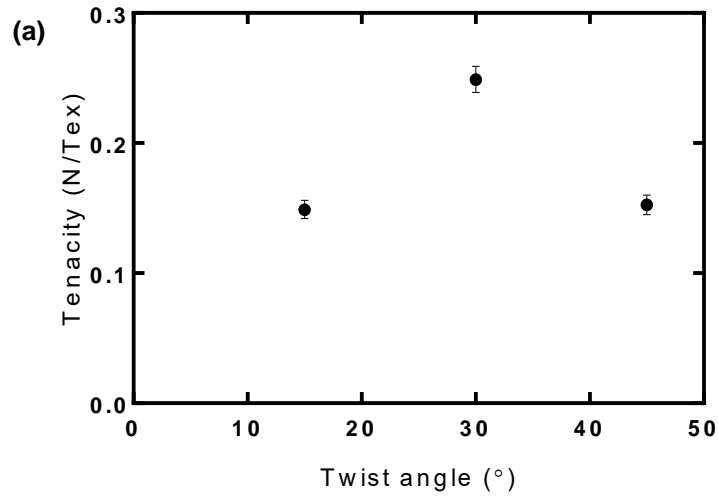


**Figure 2.** (a) Strength-twist relationship of CNT yarn. (b) Schematic of the strength-twist relationship for textile yarn, depicting the mechanisms of the association. (c) Flyer-spun CNT yarn tenacity as a function of twist.

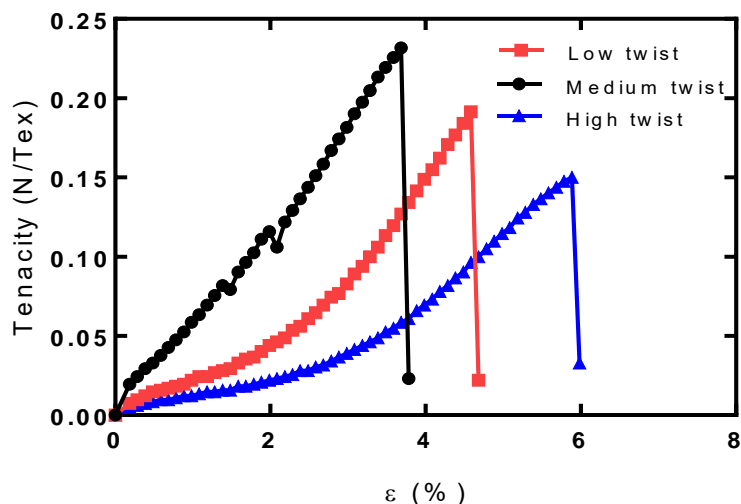


**Figure 3.** Tenacity-strain curves for different twist levels.

*Mechanical Properties: Toughness* [8, 30]. Unlike in strength measurements, the highest value of volumetric toughness ( $4.7 \text{ MJ m}^{-3}$ ), was observed in the high twist CNT yarns (Figure 4). It was then, followed by the medium twist ( $3.6 \text{ MJ m}^{-3}$ ) and lastly the low twist CNT yarns ( $2.3 \text{ MJ m}^{-3}$ ). The toughness of the CNT yarns increases with twist level. Although medium twist CNT yarns showed the highest strength, their low strain values, brings about a relatively lower toughness to the high twist CNT yarn. The gravimetric toughness follows the same pattern as the volumetric toughness, with the least value of gravimetric toughness ( $6.5 \text{ J g}^{-1}$ ) obtained at low twist and the highest value at high twist ( $8.7 \text{ J g}^{-1}$ ). Toughness of CNT yarn is strongly dependent upon the alignment of CNTs in the axial direction of the yarn. Since coherency of fiber bundles in the yarn increases with twist level, it is expected that increased degree of packing leads to increased toughness. However, improving toughness in CNT yarns can be challenging. This is because it is difficult to produce a very strong yarn that can withstand a significant amount of strain. While increasing the twist level can help with elongation, large stress at high twist (above the optimum) decreases the tensile strength. However, the medium twist CNT yarn showed the highest tensile factor of 0.43 compared to the 0.31 and 0.36 obtained for the low and high twist CNT yarns, respectively. The tensile factor provides a better insight into the resilience of the yarn. This makes a medium twist better in absorbing elastic energy. Since tougher yarns provide better resistance to elastic and plastic deformations, they are

mechanically suitable for extreme environmental conditions including impact, shock and vibrations. They can be incorporated into flexible and stretchable smart textiles.

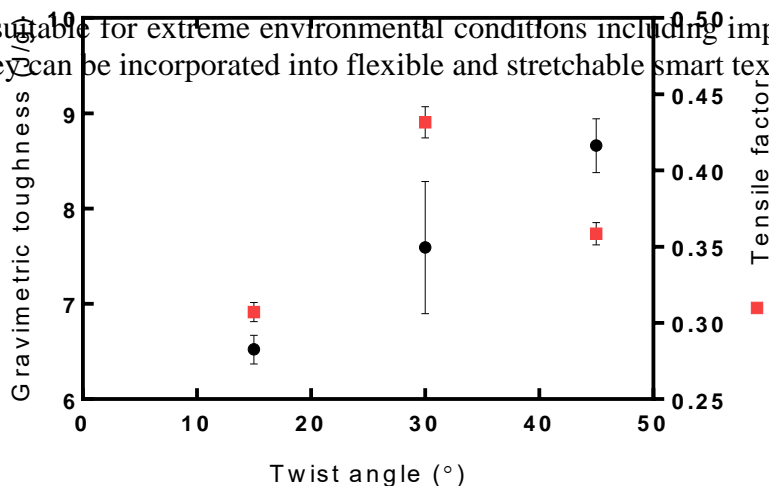


**Figure 4.** Gravimetric toughness and tensile factor versus twist for CNT yarn.

#### Electrical Properties [8, 30]

Porosity and diameter of the CNT yarn are functions of the twist as seen in Figure 5a. CNT yarns spun directly from an array are generally porous. Twist insertion in strengthening dry spun CNT yarn, achieves that purpose by binding the fiber bundles together. The decrease in diameter with increasing twist is due to the increased tension from the outside to the interior of the yarn as twist increases. The higher the twist, the higher the tensions that is exerted on the yarn. This axial tension creates a counteracting lateral compressive force on the yarn which increases the packing density. As the fiber bundles condenses in the yarn, the diameter of the yarn decreases. Solvent densification, by shrinking the yarn, achieves the same purpose. This condensation process reduces the pore size in between the fiber bundles and more importantly, brings the CNTs in the bundles closer.

Bearing in mind that tunnel junctions are significant to electron transport in CNT yarns, this increased packing density obtained at higher twist explains the increase in conductivity of CNT yarns. An inverse relationship of the porosity of the CNT yarn to the twist angle (Figure 5a), and of the conductivity of the CNT yarn to the porosity (Figure 5b), means that when CNTs are closely packed in the yarn, electron mobility is more efficient, increasing the conductivity of higher diameter and have less variation of mass or

linear density, the observation is accurately explained by the porosity of the CNT yarn. The electrical conductivity of the flyer-spun twisted and twist-untwisted yarns as shown in Figure 5c, increased rapidly as the level of twist increased.

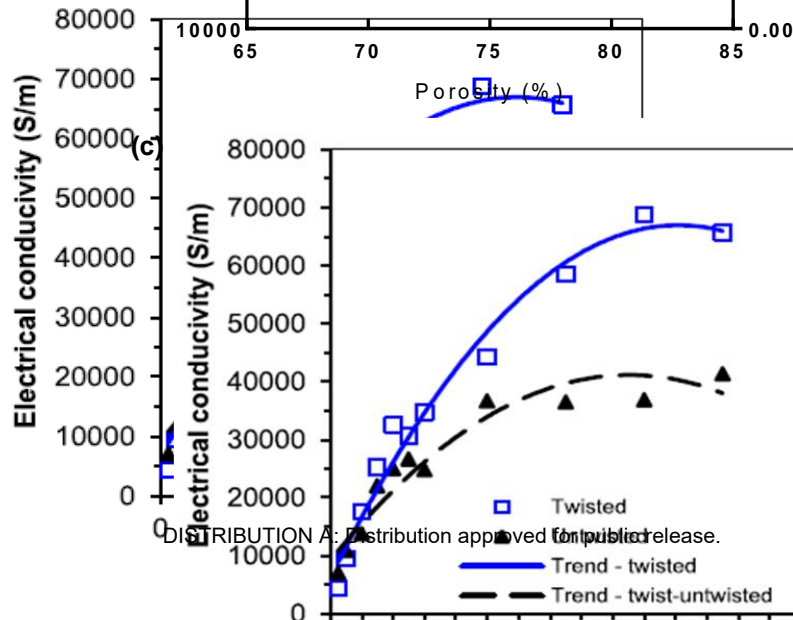
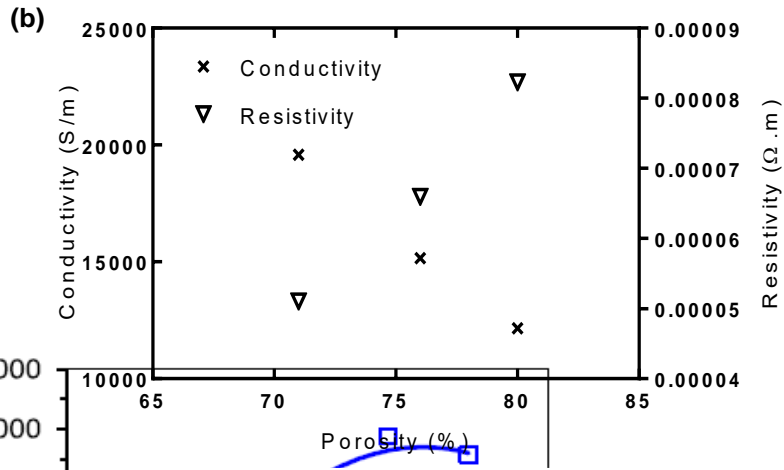
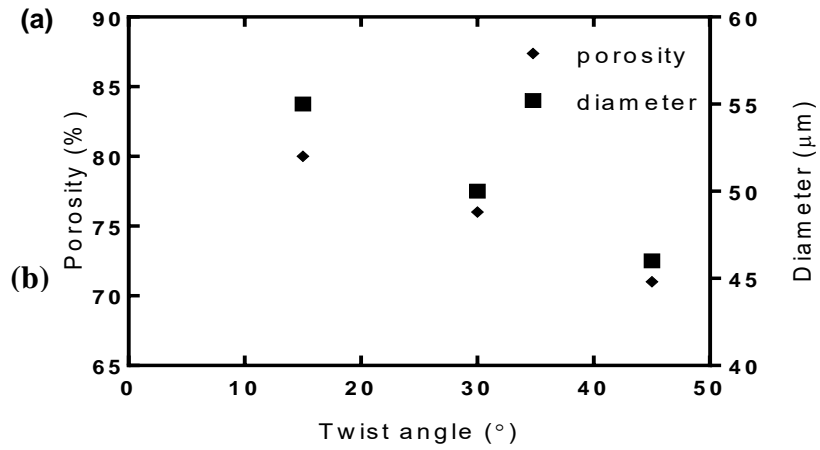


**Figure 5.** (a) Porosity and diameter of the CNT yarn versus twist angle. (b) Conductivity and resistivity of the CNT yarn versus porosity. (c) Electrical conductivity of flyer-spun twisted and twist-untwisted CNT yarns as a function of twist.

Piezoresistivity [8, 30]

CNTs are known to exhibit ballistic conductivity due to minimal electron scattering in their 1-D structure with mean free paths of the order of tens of microns. Under deformation, the charge carriers are separated leading to an increase in resistance. For very small strains, the deformation has shown to be elastic and the conductive network is fully recovered when the strain is removed, leading to a decrease in resistance. Plastic deformation however, has proven to be different. Although the resistance goes to zero when the strain is removed, hysteresis has been observed. The piezoresistivity of CNT yarns comes from two types of resistance changes: (1) The intrinsic resistance of the carbon nanotubes; and (2) the inter-tube resistance of nanotubes in proximity or contact. The intrinsic resistance,  $R_i$ , is the resistance of the CNT yarns due to the stretching of their carbon to carbon (C-C) bonds or separation of their charge carriers. The inter-tube resistance is broken down into contact resistance,  $R_C$ , of nanotubes in physical contact or tunneling resistance,  $R_T$ , when nanotubes are separated by small gap. The tunneling resistance is expressed as:

$$R_T = \frac{dh^2}{Ae^2\varphi} e^{\frac{4\pi d}{h}\varphi} \quad (3)$$

where  $d$  is the tunneling distance between CNT,  $h$  is Planck's constant,  $A$  is the effective cross-sectional area,  $e$  is the quantum of electricity, and  $\varphi$  is given by:

$$\varphi = \sqrt{2m\delta} \quad (4)$$

where  $m$  is the electron mass, and  $\delta$  is the height of the potential barrier between adjacent CNTs. From Eq. (3),  $R_T$  increases nonlinearly, resulting in a nonlinear piezoresistivity.

Inter-tube resistance is higher in CNT yarns due to the number of CNTs in contact. The short or discrete length of the CNTs means that junction resistance will play a part in their piezoresistivity under axial strain. Considering that CNTs do not span the entire length of the fiber, intrinsic resistance is expected to play a minimal role in the piezoresistive response and it can be concluded that the piezoresistivity of CNT yarns are inter-tube resistance-driven. Increase in CNT length will increase the contribution of intrinsic resistance in the yarn and reduce the effect of inter-tube resistance due to contact. When a free or neat CNT fiber is stretched, we expect the deformation mechanism is dominated by: (1) breaking of contact due to fiber unraveling and bond breaking; (2) slippage. The first phenomenon leads to an increase in contact resistance. In the presence of a matrix,

tunneling seems to drive the piezoresistivity due to matrix infiltration of the porous fibers creating barriers for electron tunneling to occur.

For a strain gauge, the sensitivity is represented by the ratio of relative change in electrical resistance  $\Delta R/R_0$ , to the mechanical strain

The sensitivity of the CNT yarn represented by the gauge factor is given as:

$$GF = \frac{\Delta R/R_0}{\epsilon} = \frac{\Delta R/R_0}{\Delta L/L_0} \quad (5)$$

where  $R_0$  is the initial resistance,  $\Delta R$  is the change in resistance,  $\epsilon$  is strain, which is defined as the ratio of the change in length  $\Delta L$  over the original length  $L$ . Although the GF for SWCNT-based piezoresistive strain sensors have been shown to be greater than 2900, CNT-fiber based sensors have shown values lower than that. The reported gauge factor of neat CNT yarns was around 0.5. The dominance of contact resistance between CNT bundles in the yarn means that the contribution of intrinsic resistance in the individual CNTs is minimal in a CNT yarn.

#### Integrated Damage Detection in Composite Materials Using CNT Yarns and Validation [7, 30, 31, 33]

Experimental studies had been conducted to evaluate the ability of piezoresistive-based, integrated and distributed, carbon nanotube yarn sensors to detect incipient damage and delamination in laminated composite materials, determine the specific location of the damage and delamination, and further understand the yarn sensors' response in this monitoring methodology. The study included monitoring the growth of preset delamination defects and randomly appearing damage during loading of glass fabric polymeric laminated composite samples using integrated yarn sensors. The study demonstrated the ability of the yarn sensors to not only capture the delamination but also anticipate it as exhibited by a significant increase in the resistance of the stitched yarn sensors ahead of the delamination. The sensitivity of the yarn sensors is also exhibited by their ability to detect minor damage as demonstrated by a slight increase in their resistance immediately after the load experiences a small reduction. Despite the sensitivity of the integrated yarn sensors, they can sustain significant deformation and fail, as exhibited by their resistance increase to infinity, when the host laminated composite fails. The exact location and progression of a delamination was determined by additional straight yarn sensors that yield a higher resistance output when the delamination reaches their specific locations. All these findings continue to demonstrate the feasibility of a multi-sensor network of integrated and distributed carbon nanotube yarn sensors to monitor an entire designated area and pinpoint the exact location of damage. These carbon nanotube yarn sensors provide excellent piezoresistive response to loading without compromising the integrity of the laminated composite, offering thus the potential for developing a highly adaptive, practical, and sensitive structural health monitoring technique. Figure 6a shows the layout of the integrated CNT yarn sensors, while Figure 6b shows an optical image of the actual sample and Figure 6c shows the schematic of the sample and the loading pattern. Figure 7 shows the experimental results of the testing of a laminated composite sample subjected to bending and instrumented with both stitched and straight CNT yarn sensors that can capture the presence of delamination in real time and indicate its exact location and progression.

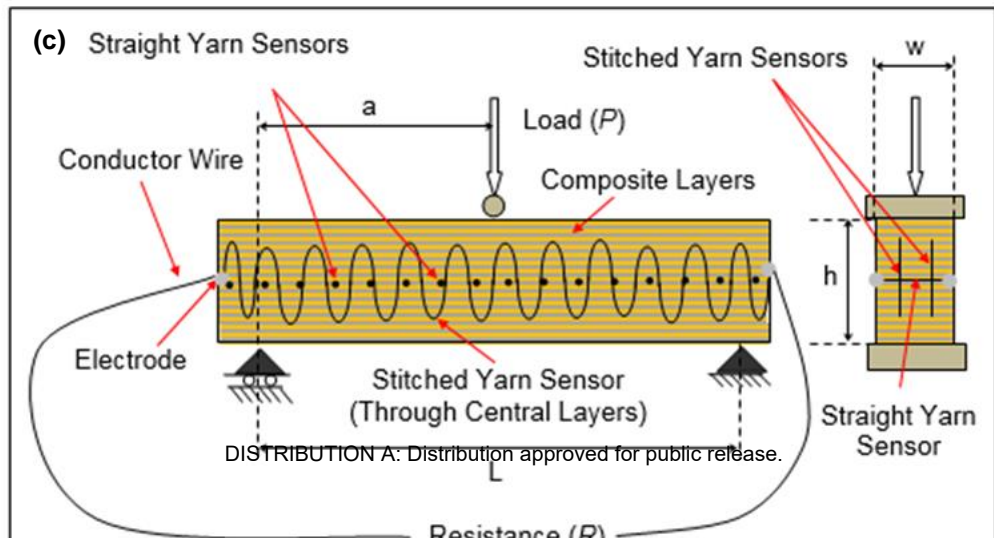
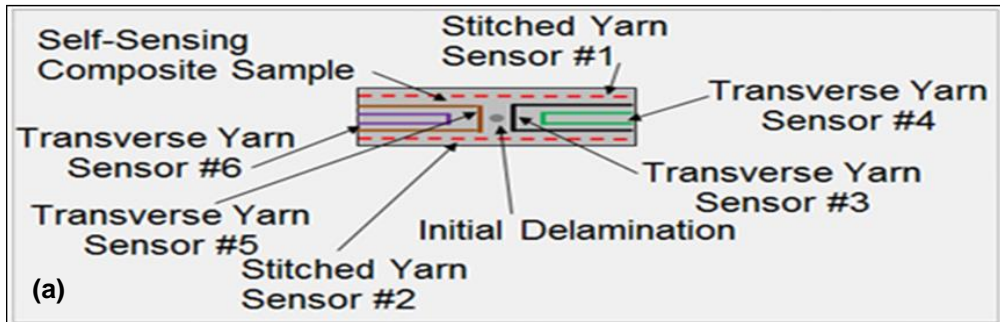


**Figure 6.** Schematic of a 32-layer glass/epoxy laminated composite of the integrated yarn sensors including stitched ones (through layers 12-21) and straight ones (between layers 16 and 18), with a 25 x 15 mm central delamination. Wires are later connected to the CNT yarns for resistance measurements. (b) Optical image of the laminated composite samples instrumented with CNT yarn sensors and multimode fiber optic sensor. (c) Schematic of experimental setup of self-sensing composite sample subjected to 3-point bending: side and end cross-sectional views of laminated composite beam sample instrumented with stitched and straight yarn sensors.

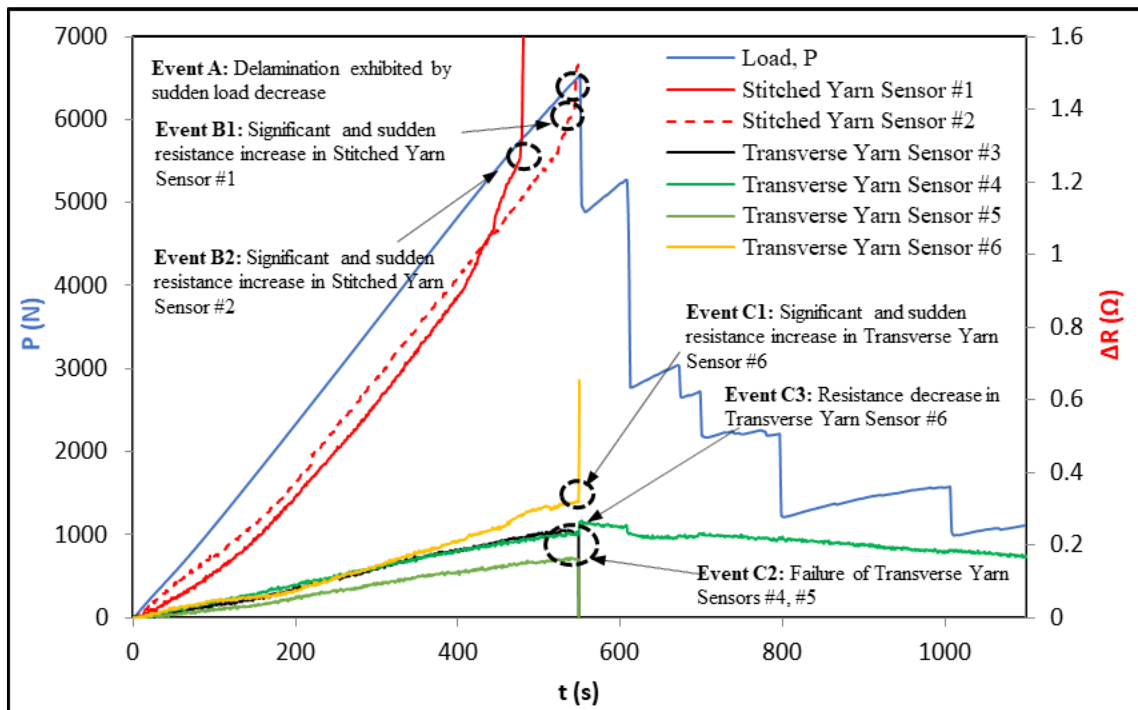


**Figure 7.** Localized detection of major delamination in 6-layer glass/epoxy composite sample using a combined stitched and straight yarn sensors configuration: load and delta resistance versus time curves.

Figure 8 shows the schematic of the samples that include integrated optical fiber sensors. Initially, multimode plastic fibers, are being stitched and integrated through the structure to corroborate through photon counting of the backscattered signals, the presence of damage indicated by the CNT yarn sensors. For the first sample test, the previous experimental results obtained with the CNT fiber sensors have been validated using integrated optical fibers. The simultaneous validation of the CNT yarn sensor data was performed by using an optical time domain reflectometer (OTDR) and a photodiode. In the scope of this study, the v-OTDR device has used for locating the damage along a 105  $\mu\text{m}$ -diameter multimode plastic optical fiber integrated in a composite sample as seen in the damage point at Figure 9. It shows the resistance change of the two CNT yarn sensors and the voltage change of the photodiode versus time. The first CNT yarn has failed at 274 s, while the second CNT yarn failed damage at 484 s. Voltage from photodiode that was contactor by fiber optic was the first one which fielded of sample. The voltage data indicates that the fiber optic failed at 269 s. There are differences in the results between CNT yarn 1, CNT yarn 2, and fiber optic. The fiber optic made of glass and it is thicker than CNT yarn 1,2 which makes it get the pressure and damaged first.

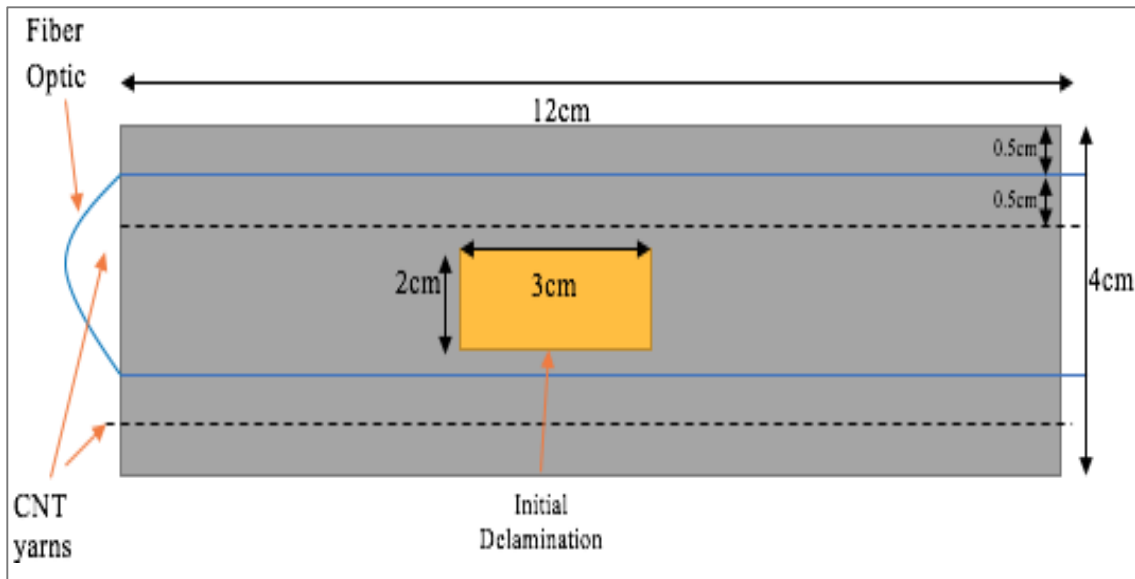


**Figure 8.** Schematic of composite sample including stitched and transverse CNT yarn sensors and plastic optical fiber sensors.

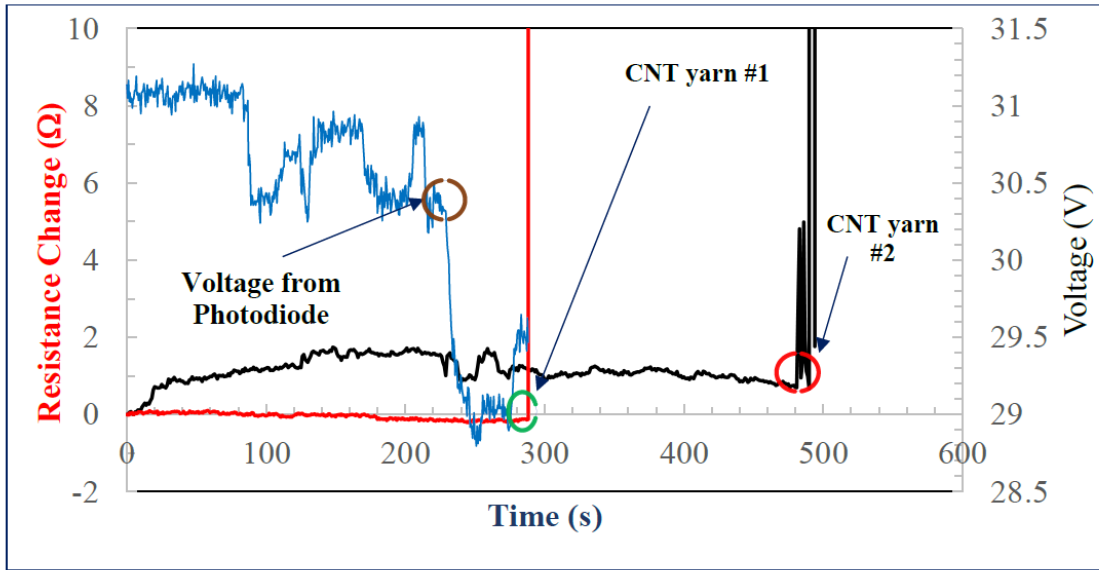
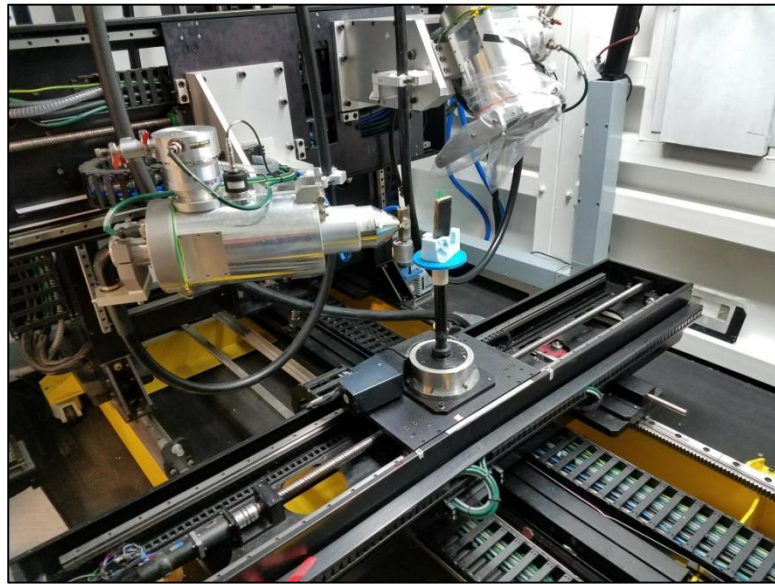


**Figure 9.** Resistance change from CNT yarns and voltage from photodiode indicating the failure captured by each sensor.

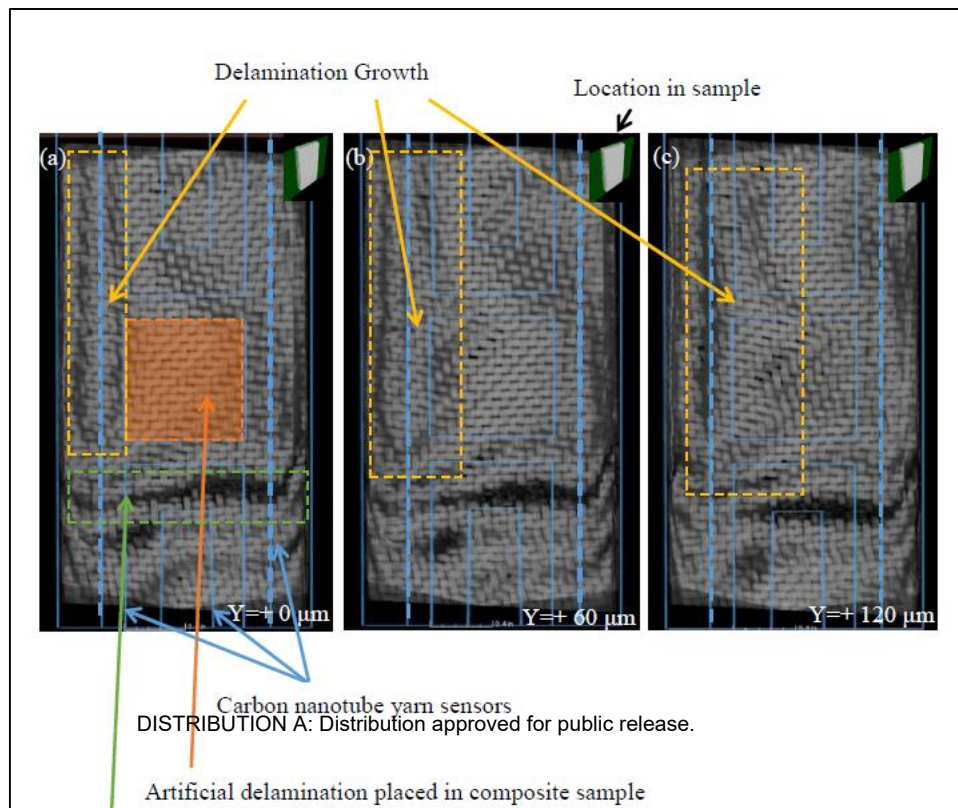
X-ray micro-tomography is a technique used to nondestructively characterize material microstructure in three dimensions at a micron level special resolution. The objective of this study was to experimentally validate the prediction of damage by the carbon nanotube yarns that were embedded in a laminated composite sample and which were subjected to a three-point bending test hence providing the location of where the delamination occurred. The experiments included the use of x-ray micro-tomography to obtain high resolution three dimensional images of a composite sample and providing the exact location and the extent of delamination in the sample. These x-ray tomography images were not only able to capture the delamination and damage but could also detect the presence of carbon nanotube yarns inside the sample. Thus, the results obtained with the carbon nanotube yarn sensors were corroborated by an in-situ experimental technique and using a post-test imaging technique that validated the damage location as predicted by the carbon nanotube yarns. Figure 10 shows the experimental setup of the composite sample in the x-ray device (Nikon 225kv Micro-Focus CT/X-Ray system from Chesapeake Testing).

Figure 11 shows images taken at every 60  $\mu\text{m}$  in the center of the sample. The blue schematic is the schematic of the layout of the carbon nanotube yarns in the sample that has been overlaid over the x-ray micro tomography images. The arrows draw attention to significant parts of the image. The orange arrow points toward the artificial delamination, the green arrow shows damage that occurred to the sample presumably during the bending test, and the yellow arrow shows what is believed to be the propagation of delamination through the sample. The reason that the delamination in the sample is believed to propagate is because if the region (that the yellow arrow is pointing toward) is observed as the image

is resolved, the direction of the glass fiber weave changes. Through a range of about 420  $\mu\text{m}$ , we can observe a layer that sits diagonally along the center of the sample, which is why it is not visible in one image as bits of this layer emerge in different layers of the sample. This delamination originates from the artificial delamination placed in the sample at the time of fabrication. In Figure 11a, it can be observed that the glass fiber weave for the most part is flat, but from Figure 11b-c, the propagation of delamination is visible as a layer of glass fiber at an angle all the way until where another flat layer starts becoming visible.



**Figure 10.** Optical image of composite sample positioned in front of CT/X-ray system in a foam cradle.



**Figure 11.** (a-c) Collection of images superimposed with a schematic of the composite sample showcasing the damage propagation through the composite sample. The colored arrows show areas of interest.

Strain Measurement Using CNT Yarn Sensors [2,6]

A schematic of the strain gauge sensor configuration including the piezoresistive layer containing the CNT yarns, the substrate composed of a polymeric material, and the electrodes is shown in Figure 12. The “building block” or basic initial configuration of the piezoresistive layer is an arrangement of parallel CNT yarns as shown in the inset of Figure 12. The modeling of the piezoresistive response of the strain gauges had indicated that their sensitivity would be sufficient to measure strain and that the gauge factor could potentially reach higher values than those of metallic foil strain gauges. The strain gauge substrates (Figure 13a-d) were fabricated at the University of São Paulo and the first strain gauge prototype was now fabricated at Catholic (Figure 13e).

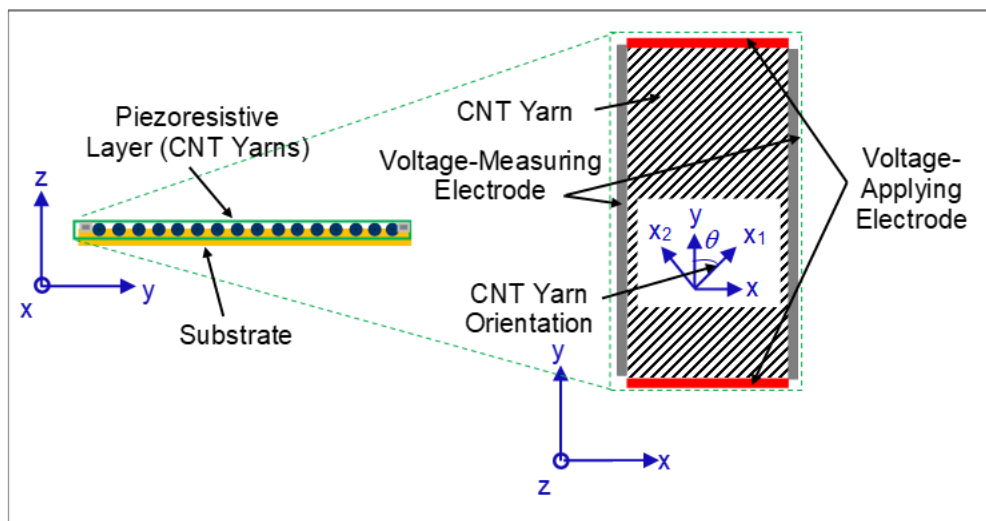


**Figure 12.** Schematic of cross-section of the foil strain gauge sensor comprising CNT yarns. Inset: top schematic view of the arrangement of the CNT yarns in a unidirectional configuration.

The experimental results include the correlation of the strain data from the metallic foil strain gauge and the resistance data of the foil strain gauge prototype (Figure 14). Figure 14a shows the applied strain and relative resistance change histories. The relative resistance change data was noise-reduced and smoothed using digital non-linear filters and curve fitting models on Excel™ and Matlab™. The relative resistance change history curves indicate that the foil strain gauge sensor prototype is responsive to the loading and exhibits a cyclic response that mimics perfectly that of the applied strain history. The duration of each cycle is identical to that of the applied strain cycle (obtained from the strain history of the metallic foil strain gauge) and no lag in the response of the foil strain gauge is consistently observed in each cycle, as shown in Figure 14. In the case of the experiments at 300  $\mu\text{m}/\text{min}$  ( $5.5 \times 10^{-5} \text{ s}^{-1}$ ), the relative resistance change reaches about 1% for about 0.04%-strain levels. Towards their fourth cycles, a slight decrease in the piezoresistive response of the strain gauge prototype was observed in Figure 14. As the same foil strain gauge prototype was immediately subjected to additional cyclic loading, it was observed that the gauge would not recover completely exhibiting a non-zero resistance.

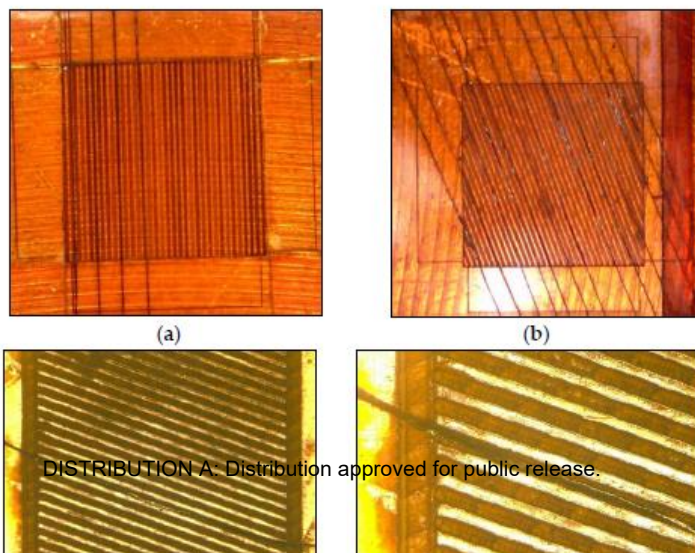
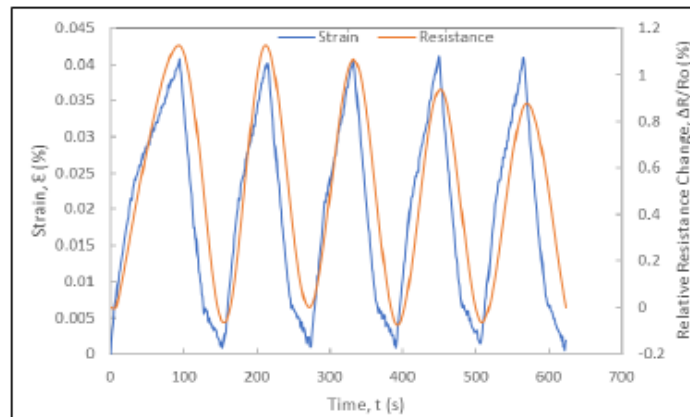


**Figure 13.** Optical images of the foil strain gauge prototypes: (a) Substrate with several CNT yarns placed in the grooves at 0°-inclination; (b) Substrate with several CNT yarns placed in the grooves at 70°-inclination. (c) Substrate with a CNT yarn placed in the groove; (d) Close-up of the substrate with a single CNT yarn placed in the groove; (e) Complete gauge showing CNT yarns in the grooves, adhesive layer on the gauge area, and conductive silver on the electrodes.



DISTRIBUTION A: Distribution approved for public release.

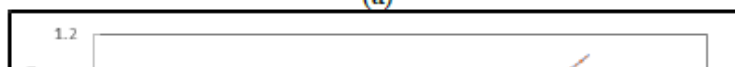


**Figure 14.** Electromechanical response of a foil strain gauge prototype under cyclic loading at a displacement rate of 300  $\mu\text{m}/\text{min}$ : (a) Strain and relative resistance change histories during five loading-unloading cycles; (b) Relative resistance change versus strain curve of first loading cycle and corresponding gauge factor.

Temperature Measurement Using CNT Yarn Sensors [15]

Initial studies are being conducted to understand the thermo-piezoresistive response of CNT yarns to develop thermistors and decouple temperature effects from strain measurements in foil strain gauges. The thermoresistivity of the CNT yarn and the CNT yarn embedded in a Vinylester polymer is shown in Figure 15. The former exhibits a linear response, higher sensitivity, positive residual resistance and lower hysteresis. The latter exhibits a nonlinear response, lower sensitivity, negative residual resistance and higher hysteresis. It was concluded that the sensitivity reduced, and that hysteresis increased by the confinement provided by polymer matrix.

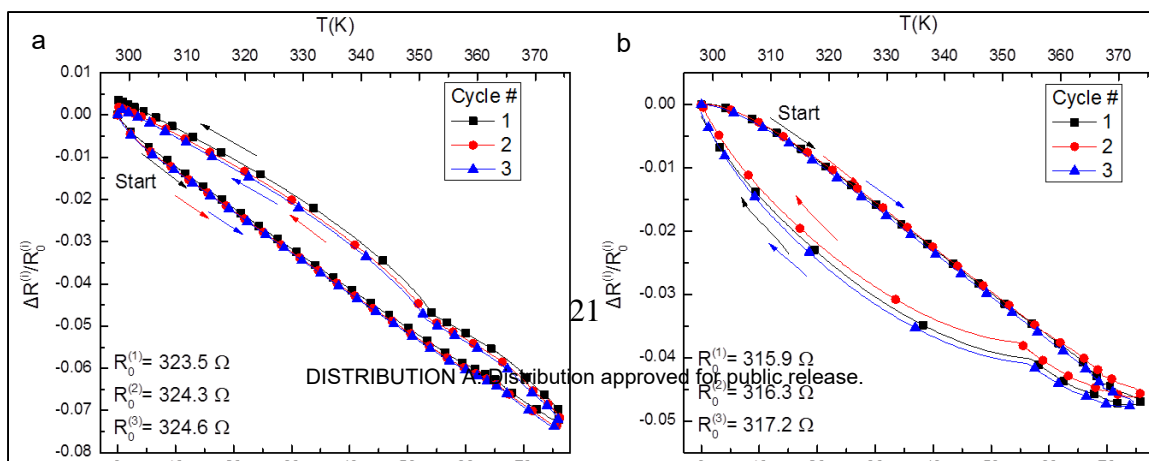


**Figure 15.** Thermoresistive of: (a) CNT yarn. (b) CNT yarn embedded in vinyl ester polymer.

#### Torque Sensors Using CNT Yarns [14, 30]

Most applications that require rotational positioning and high torque generation for mechanical performance are often non-compact with a complex design that is not ideal for nanotechnological applications. Twist-spun CNT yarn can serve as an actuator for high-performance motion systems like artificial muscles that require torsional rotation in addition to bending and contraction and micromechanical devices. In addition to their relatively high strength, their nanoscale dimensions and aspect ratio are attractive for torsional sensing. Torsional acceleration in CNT yarns can be driven in both directions for conversion of mechanical energy to electrical energy. This can find application in sensors that generate electrical signals through applied torsional rotation. To demonstrate the torsional applications of CNT yarns, a simple oscillations set-up was designed using a pendulum. The experiments were conducted to measure the change in resistance of the CNT yarn relative to the angular displacement. The decrease in electrical resistance upon application of torsional loading to the CNT yarns demonstrate that applied twist increases fiber compaction, resulting in increased electrical contact between nanotubes and a negative piezoresistance (Figure 16 with a twist angle of  $20^\circ$ ). When the twist is reversed in the opposite direction to the angle of twist, fiber unraveling could be initiated and, a positive piezoresistivity is observed. Since it is difficult to observe the twist direction in the CNT yarn with the naked eye, the sign of the piezoresistivity acts as an indicator to the direction of the torsion on the yarns.

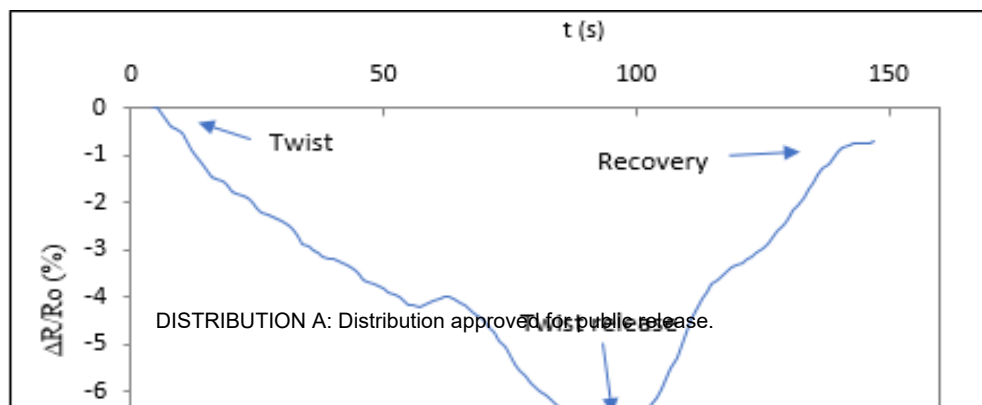


**Figure 16.** Changes in electrical resistance  $R$  (normalized), due to the CNT yarn twist. Twisting initiates at  $t=0$ , then  $R$  changes due to applied shear strain in the fiber. Strain in the yarn are released by counter-rotation of the disk to equivalent angle for low displacement rate.

#### Wearable Sensors Using CNT Yarns [14, 30]

CNT stretchable sensors could also be developed for flexible functional electronic devices. The CNT yarn used in this study was embedded completely into the Ecoflex substrate. This configuration will prevent the CNT yarn from any form of deterioration due to harsh use or weather. The curve of the first sensor tested (sensor 1) shown in Figure 17a shows that the CNT yarn-Ecoflex™ sensor could measure strains greater than 40 %. A second sensor made with Ecoflex™ gel (sensor 2) measured up to 25 %-strain before latency to further strain (Figure 17b). By bonding them to the surface, there is a possibility that the CNT fiber is not sensitive enough to the strain in the device because it was bonded to the surface, and hence is only capable of surface strain measurement. This is possible when considering the difference in the GF reported by the authors to that of this study. A stable interface between different components also plays a critical role as minute interfacial sliding or debonding may lead to failure of the entire device. The non-linear resistance change-strain curves obtained for all sensors implies that the sensitivity differs with strain levels. The CNT yarn strain sensor was used to demonstrate this motion monitoring capability by attaching them to body parts to measure movements or motion. The sensor was used to measure pinch, touch, wrist motion (Figure 17), and index finger knuckle arching movement.



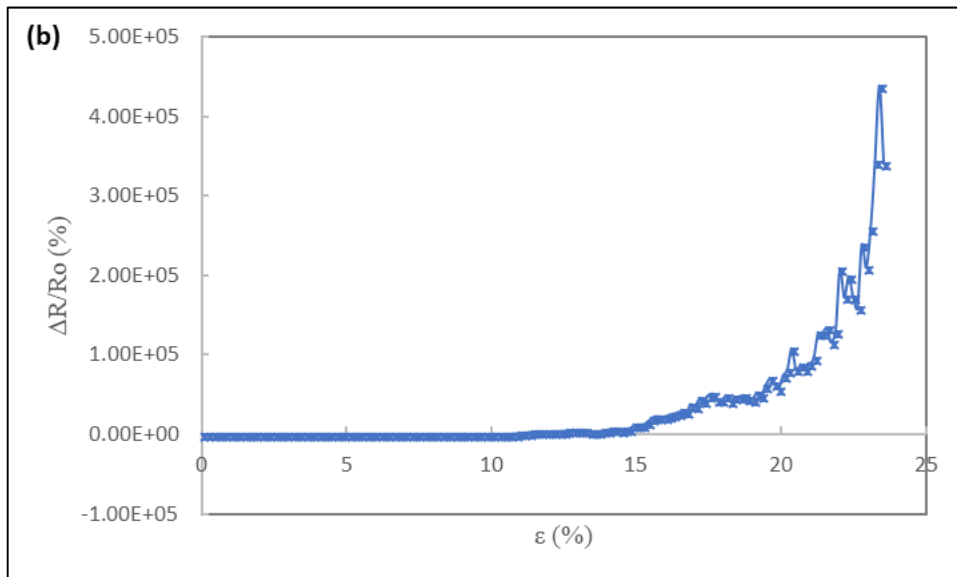


**Figure 17.** The relative resistance-strain curves for: (a) Ecoflex strip sensor 1. (b) Ecoflex strip sensor 2.

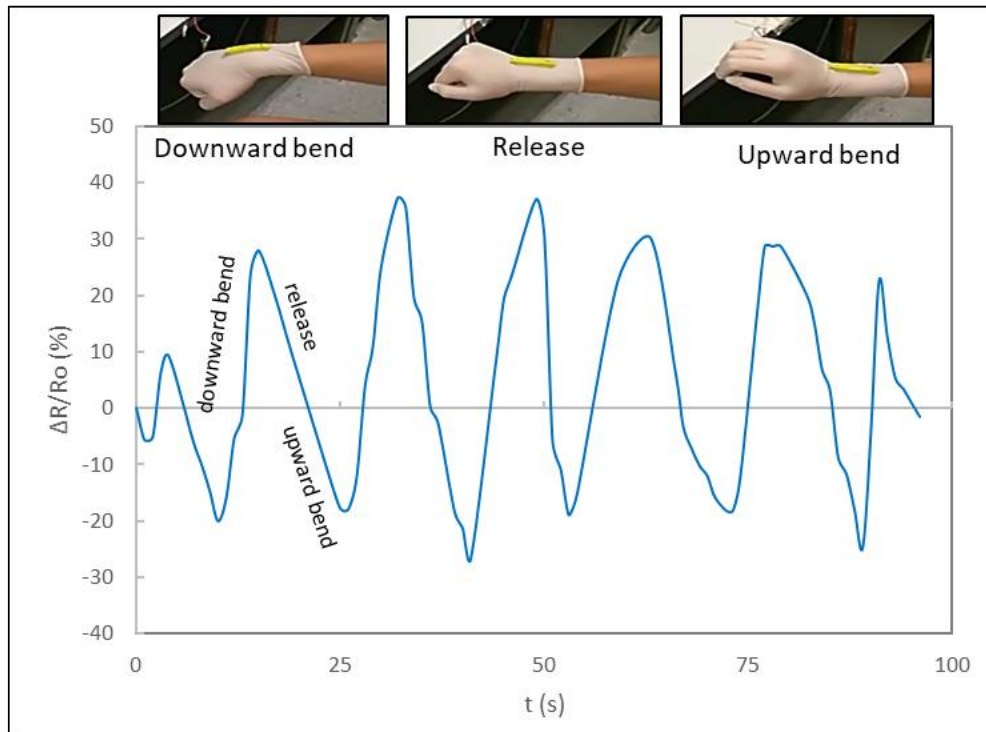


**Figure 18.** Relative resistance change-time curves for wrist motion in the case of slow bend motion.

### Personnel Supported (2017-2018)

The following researchers were supported to accomplish the objectives in this project.

1. Kalayu Belay (PI of FAMU)
2. Estrella Jhorkys (Undergraduate student of FAMU)
3. Jandro Abot (PI of subcontract at Catholic)
4. Jude Anike (graduate student at Catholic)\*
5. Tannaz Tayyarian (graduate student at Catholic)\*
6. Binita Saha (graduate student at Catholic)\*
7. Abdulrahman Binfaris (graduate student at Catholic)\*
8. Joseph Bills (undergraduate student at Catholic)
9. Grace Brodeur (undergraduate student at Catholic)
10. Lauren Coene (undergraduate student at Catholic)
11. Kevin Albin (undergraduate student at Catholic)
12. Brennan Woo (undergraduate student at Catholic)\*
13. Zachary Onorato (undergraduate student at Catholic)\*
14. Gregory Van Roie (undergraduate student at Catholic)\*
15. Elizabeth Jean (undergraduate student at Catholic)\*
16. Joseph Allan III (undergraduate student at Catholic)\*

\* Contributed to this project with support from other sources at Catholic.

## Equipment Acquisition

A new modern 850 Dynamic Mechanical Analyzer (DMA) was purchased and installed in the Carbon-Based Materials Lab, at The Center for Plasma Science and Technology (CePaST) housed in the Florida A&M University, Centennial Building located in the Innovation Park (2077 E. Paul Dirac Dr, Tallahassee, FL 32310).

## Publications (2015-2018)

### Journal Papers

1. Anike, J. C., Belay, K. and Abot, J. L. Effect of twist in the electromechanical properties of carbon nanotube yarns. *Carbon* (accepted for publication).
2. Abot, J. L., Góngora-Rubio, M. R., Anike, J. C., Kiyono, C. Y., Mello, L. A. M., Cardoso, V. F., Rosa, R. L. S., Kuebler, D. A., Brodeur, G. E., Alotaibi, A. H., Coene, M. P., Coene, L. M., Jean, E., Santiago, R. C., Oliveira, F. H. A., Rangel, R. C., Thomas, G. P., Belay, K., da Silva, L. W., Moura, R. T., Seabra, A. C. and Silva, E. C. N. Foil strain gauges sensing using piezoresistive carbon nanotube yarn: Fabrication and calibration. *Sensors Special Issue: Integrated Structural Health Monitoring in Polymeric Composites* 18, 464 (2018).
3. Anike, J. C., Belay, K. and Abot, J. L. Piezoresistive response of carbon nanotube yarns under tension: Parametric effects and phenomenology. *New Carbon Mater.* 33 (2):140-154 (2018).
4. Anike, J. C., Le, H. H., Brodeur, G. E., Kadavan, M. M. and Abot, J. L. Piezoresistive response of integrated carbon nanotube yarns under compression and tension: the effect of lateral constraint. *J. Carbon Res.* 3, 14 (2017).
5. Anike, J. C., Bajar, A. and Abot, J. L. Time-dependent effects on the coupled mechanical-electrical response of carbon nanotube yarns under tensile loading. *J. Carbon Res.* 2(1), 3 (2016).
6. Abot, J. L., Kiyono, C. Y., Thomas, G. P. and Silva, E. C. N. Strain gauge sensors comprised of carbon nanotube yarn: Parametric numerical analysis of their piezoresistive response. *Smart Mater. Struct.* 24 (7): 075018 (2015).
7. Abot, J. L., Wynter, K., Mortin, S. P., Borges de Quadros, H., Le, H. H., Renner, D. C. and Belay, K. Localized detection of damage in laminated composite materials using carbon nanotube yarn sensors. *J. Multifunc. Compos. Special Issue: Novel Sensing Techniques and Approaches in Composite Materials 2*: 217-226 (2014). Published in 2016.

### Book Chapters

8. Abot, J. L. Chapter 10: Strain Measurement and Structural Health Monitoring using Anike, J. C. and Abot, J. L. Chapter 11: Sensors Based on CNT Yarns and CNT-Reinforced Nanocomposite Fibres, *Carbon Nanotube Fibres and Yarns - Production, Properties and Applications In Smart Textiles*, edited by M. Miao, Elsevier, ISBN TBD (2018).

9. Anike, J. C. and Abot, J. L. Chapter 4.4: Carbon Nanotubes and Carbon Nanotube Fibers, *21<sup>st</sup> Century Nanoscience – A Handbook*, vol. 4, edited by K. Settler, Taylor & Francis, ISBN TBD (2018).
10. Abot, J. L. Chapter 10: Structural Health Monitoring Using Integrated Carbon Nanotube Fibers, *Nanotube Superfiber Materials, Science to Commercialization*, vol. 2, edited by M. J. Schulz, Elsevier, ISBN TBD (2018).
11. Abot, J. L. and Punnakattu Rajan, C. Chapter 14: Carbon Nanotube Fibers, *Carbon Nanomaterials Sourcebook*, vol. 1, edited by K. Settler, Taylor & Francis, ISBN 978-14-822527-2-9 (2016).

#### Conference Proceeding Papers

12. Anike, J. C., Saha, B. and Abot, J. L. Development of robust electrically insulated carbon nanotube yarns for sensing in conductive composites. *Proceedings of 33<sup>th</sup> American Society for Composites Conference, Seattle, WA* (2018).
13. Pirmoz, A., Anike and Abot, J. L. Meso-scale computational simulation of CNT yarns. *Proceedings of 33<sup>th</sup> American Society for Composites Conference, Seattle, WA* (2018).
14. Anike J. C. and Abot, J. L. Carbon nanotube fiber-based torsion sensors: effect of twist on their piezoresistivity. *Proceedings of the Materials Research Society Symposium, Phoenix, AR* (2018).
15. Balam, A., Cen-Puc, M., Gamboa, F., Abot, J. L. and Avilés, F. Thermoresistivity of polymeric composites modified with carbon nanotubes and carbon nanotube yarns. *Proceedings of ASME International Mechanical Engineering Congress & Exposition, Tampa, FL* (2017).
16. Abot, J. L., Anike J. C., Bills J. H., Onorato, Z., Gonteski, D. L., Kvelashvili, T. and Belay, K. Carbon nanotube yarn sensors for precise monitoring of damage evolution in laminated composite materials: Latest experimental results and in-situ and post-testing validation. *Proceedings of 32<sup>nd</sup> American Society for Composites Conference, West Lafayette, IN* (2017).
17. Anike, J. C., Bills, J. H., Brodeur, G. E., Kadavan, M. M., Belay, K. and Abot, J. L. Comparative study of the piezoresistivity of free and constrained carbon nanotube yarns in a medium: Effect of slippage. *Proceedings of 32<sup>nd</sup> American Society for Composites Conference, West Lafayette, IN* (2017).
18. Abot, J. L., Anike J. C., Jean, E., Brodeur, G. E., Albin, K., Kadavan, M. M., Pires, F. A., Alotaibi, A. H., Belay, K., Cardoso, V. F., Rosa, R. L. S. and Seabra, A. C. Foil strain gauge sensors of piezoresistive carbon nanotube yarn: fabrication and calibration. *Proceedings of 32<sup>nd</sup> American Society for Composites Conference, West Lafayette, IN* (2017).
19. Abot, J. L. C. Structural health monitoring using carbon nanotube yarns: sensing concept and applications in composites. *Proceedings of 5<sup>th</sup> International Symposium on Sensor Science, Barcelona, Spain* (2017).
20. Anike J. C., Abot, J. L., Bills, J. H., Gonteski, D., Kvelashvili, T., Alsubhani, M. S., Albin, K., S. P. Mortin, V. R., Gonzaga, V. C., Oliveira, G. N., Silva, P. H. R. M., Navarro, R. B. A., Barbosa, V. R., Belay, K., Behrmann, G. P. and Akay, E. Integrated

- structural health monitoring of laminated composites using carbon nanotube yarns under static loading: experimental results and validation. *Proceedings of 21<sup>st</sup> International Conference on Composite Materials, Xian, China* (2017).
21. Can-Ortiz, A., Avilés, F. and Abot, J. L. Relaxation-induced piezoresistivity in carbon-based monofilament hierarchical polymer composites. *Proceedings of 21<sup>st</sup> International Conference on Composite Materials, Xian, China* (2017).
  22. Abot, J. L. and Anike, J. C. From carbon nanotube yarns to fibers into sensors: Recent findings and challenges. *8<sup>th</sup> International Conference on Nanotechnology, University of Cambridge, Cambridge, United Kingdom* (2017).
  23. Abot, J. L. Carbon nanotube fibers: Unveiling their piezoresistive response towards integrated sensing in engineering applications. *Nanotechnology Materials and Devices, Dayton, OH* (2016).
  24. Can-Ortiz, A., Ku-Herrera, J. J., Rodríguez-Uicab, O., May-Pat, A., Gamboa, F., Abot, J. L. and Avilés, F. Self-sensing of viscoelastic phenomena in multiscale composites by using the electrical resistance approach. *Proceedings of 31<sup>st</sup> American Society for Composites Conference, Williamsburg, VA* (2016).
  25. Le, H. H., Carvalho, G. L., Bonardi, M. K., Coelho, R. C., Brodeur, G., Cen-Puc, M., Ku-Herrera, J. J., Avilés, F. and Abot, J. L. Piezoresistive and thermoresistive response of constrained carbon nanotube yarns towards their use as integrated sensors. *Proceedings of 31<sup>st</sup> American Society for Composites Conference, Williamsburg, VA* (2016).
  26. Anike, J. C., AlHamdan, K., Belay, K. and Abot, J. L. Piezoresistive response of carbon nanotube yarns: Experimental characterization and phenomenology. *Proceedings of 31<sup>st</sup> American Society for Composites Conference, Williamsburg, VA* (2016).
  27. Abot, J. L., Anike, J. C., Mortin, S. P., Bills, J., Gonzaga, V., Oliveira, G., Silva, P., Araujo, R., Barbosa, V., Akay, E. and Belay, K. Precise monitoring of damage evolution in laminated composite materials using integrated carbon nanotube fiber sensors: experimental results and validation. *Proceedings of 31<sup>st</sup> American Society for Composites Conference, Williamsburg, VA* (2016).
  28. Bajar, A., Anike, J. and Abot, J. L. Hysteresis and time-dependent effects on the coupled mechanical-electrical response of unconstrained carbon nanotube fiber subjected to uniaxial tensile loading. *Proceedings of 30<sup>th</sup> American Society for Composites Conference, Lansing, MI* (2015).
  29. Abot, J. L., Wynter, K., Mortin, S. P., Le, H. H., Borges de Quadros, H. and Casarotto, V. A., Burns, J., Leo, A., Belk, A. and Belay, K. Localized damage detection and strain measurement in laminated composite materials using integrated carbon nanotube yarn sensors. *Proceedings of 20<sup>th</sup> International Conference on Composite Materials, Copenhagen, Denmark* (2015).

Dissertations/Theses

30. Jude Anike. Dissertation Title: *Carbon Nanotube Yarns: Tailoring their Piezoresistive Response Towards Sensing Applications*. Other Committee Members: Prof. Z. Wang, Prof. J. Philip, Dr. F. Avilés (CICY Mexico). Defense Date: April 2018.
31. Abdulrahman Binfaris. Thesis Title: *In-Situ Validation of Damage Detection by CNT Yarn Sensors Using Optical Fiber Sensors*. Submission Date: April 2018.

32. Binita Saha. Thesis Title: *Polymer Coating of Carbon Nanotube Yarns for applications in Carbon Fiber-Reinforced Composites*. Submission Date: April 2018.
33. Kevin Albin. Thesis Title: *X-Ray Micro-Tomography Validation of Damage Detection using Integrated Carbon Nanotube Fiber Sensors*. Submission Date: April 2018.
34. Huy Le. Thesis Title: *Piezoresistive Response of Laterally-Constrained Carbon Nanotube Yarn under Compression and Tension Loading*. Submission Date: May 2016.
35. Abdullah Bakhshwin. Thesis Title: *Self-Sensing Composite Pipe Using Carbon Nanotubes Fiber as a Sensing Device*. Submission Date: August 2016.

#### **Other Presentations**

1. Integrated Carbon Nanotube Yarn Sensors: Unveiling Their Piezoresistivity Towards Strain Measurement and Damage Detection. First International Conference on Multifunctional Nanocarbon Fibres (MNF2018), Madrid, Spain, 06/28/2018.
2. Integrated Sensing in Structures Using Carbon Nanotube Fibers. 5<sup>th</sup> International Symposium on Sensor Science (I3S2017), Sensors for Structures, Barcelona, Spain, 09/26/2017.
3. Piezoresistive Response of Carbon Nanotube Yarns: Determining their Hierarchical Phenomenology Towards Modeling Effort. International Symposium on Multiscale Computational Analysis of Complex Materials, Lyngby, Denmark, 08/29-31/2017.
4. From Carbon Nanotube Yarns to Fibers into Sensors: Recent Findings and Challenges. 8<sup>th</sup> International Conference on Nanotechnology, University of Cambridge, Cambridge, United Kingdom, 02/26/2017.
5. Tailoring Piezoimpedance, Surface and Configurations of Carbon Nanotube Yarn Sensors for Integrated Damage Detection in Composite Materials, AFOSR Structural Mechanics Grantee Meeting, Dayton, OH, 07/14/2016.
6. Carbon Nanotube Fibers: Unveiling Their Piezoresistive Response Towards Integrated Sensing In Engineering Applications. Nanotechnology Materials and Devices, Dayton, OH, 05/24/2016.
7. Integrated and Distributed Sensing Using Carbon Nanotube Yarns: A New Paradigm in Structural Health Monitoring, Laboratory of Mechanics and Technology at École Normale Supérieure de Cachan, Université of Paris-Saclay, France, 07/17/2015.

#### **Summary of New Findings/Discoveries/Knowledge Advancement [30, 2, 8]**

1. An experimental study was conducted to determine the piezoresistive response of CNT yarns and the effect of strain rate, strain level, load transfer mechanisms and geometrical parameters on that response. The change in electrical resistance was studied as a function of strain level in CNT yarns that were subjected to uniaxial tensile quasi-static loading. As previously reported, the resistance of the CNT yarn increased with increasing strain and decreased during unloading as the material recovered its conductive structure. The change in resistance is associated with an increase in tunneling distance of charge carriers, and the inter-bundle contact of CNTs. Understanding the role slippage in the behavior of CNT yarns is crucial in optimizing their piezoresistive properties.
2. It was observed that the resistance change is associated with not only an increase in strain but also in stress. Beyond the elastic region, there is no direct proportionality of strain with stress due to effect of slippage and morphological changes. Slippage alters

the load transfer mechanism in CNT yarns creating a plastic strain that does not increase proportionally with electrical resistance. This was seen in the similarity of the hysteretic stress-strain curve to the resistance-stress hysteresis curves rather than the resistance-strain hysteresis curve at 1.5 % strain. Thus, a correlation of resistance with stress becomes more appropriate. It was observed that the hysteresis loop associated with the mechanical response of the CNT yarn is directly proportional to the strain level while the piezoresistive hysteresis is inversely proportional to the strain. Compared to the mechanical hysteresis, the unloading curve of the first cycle of the piezoresistive hysteresis appears to follow a different path, most times higher than the loading curve while the unloading curve of the mechanical hysteresis always returns to the origin.

3. Also, as previously stated in previous reports, strain rate plays a significant role in the piezoresistivity of the CNT yarn. At very low strain rates, a negative piezoresistivity was observed. This was attributed to the slippage and structure reformation of the CNT yarn. Slippage introduces uneven stress distribution, which allows the CNT yarn to reshape under load. Under this condition, the failure of the CNT yarns depends on the CNT bundles. At higher strain rates, a positive piezoresistive response was observed as the load exerted on the CNT yarn was much uniformly transferred to the structure through interfacial contacts of the CNT bundles. The resistance was monotonously proportional to the strain and stress during both loading and unloading segments.
4. It was also observed that the strain rate does not affect the gauge factor (GF) as much as the strain level does. There was in fact, very little or negligible change in the gauge factors when calculated at different strain rates. However, the gauge factors increased with increasing strain, peaking at 1-1.5 %-strain before subsiding at strains above 2 %. CNT yarn of higher cross-sectional area ( $47 \pm 4.1 \mu\text{m}$ -diameter) showed higher resistance change than those of lower cross-sectional area ( $25 \pm 5.3 \mu\text{m}$ -diameter). This may be explained by the contact nature of the resistance transfer in CNT yarns making the high-diameter yarn experience more friction under uniaxial tensile deformation. Slippage has a greater effect on shorter CNT yarns than longer ones due to less contact length in shorter yarns. Consequently, the shorter CNT yarns exhibit smaller GF.
5. The effect of twist on the electromechanical properties of multi-walled carbon nanotube yarn was also studied. The experimental results provided insights into the relative influence of parameters such as yarn twist angle, yarn volume fraction, and nanotube-to-nanotube interactions including friction developed by twist and mechanical loading on the characteristics of CNT yarn. Low twist CNT yarn experience unraveling of the twist under tension and consequently, an increase in slippage. Slippage plays an important role in load and charge transfer mechanisms in CNT yarns. High twist in CNT yarn ensures minimal slippage due to fiber compaction under tension while little or no twist produces significant slippage.
6. In terms of strength, the role of twist is to improve fiber effectiveness or the bond between fibers and their bundles through friction. In doing so, coherency (which relates to the effect of the forces of friction from the lateral pressure exerted on the yarns under axial tensile stress) is imparted into the yarn. Thus, it can be stated that twist imparts sufficient strength to the yarn to withstand strain. The tensile strength of CNT yarns increases as twist increases to an optimum twist level. This optimum twist

level for a CNT yarn was found to be around 30° angle. Beyond this optimum, fiber bundles are oriented far away from the yarn axis reducing the contribution of the fiber bundles' strength to the overall strength of the yarn. The decrease in strength with twist is associated with fiber obliquity reducing the contribution of the strength of CNT bundles to that of the CNT yarn.

7. Deformation of the CNT yarn structure bears a resemblance to that of textile yarns. The failure mechanism in uniaxial tension was found to be progressive, with the formation of fragmentation of CNT yarn into short segments whose ability to carry load was diminished as the segments approached some critical length. Careful examination of the failed yarns indicates that the failure mechanism was preceded by unraveling and dominated by slippage.
8. The higher the twist, the higher the elongation at failure. Although at the point of optimum strength, the elongation is smaller due to high tenacity. High twist provides high tensions on the yarn leading to an increase in the yarn packing density. As the packing density increases, the diameter of the yarn reduces, which also reduces the porosity. Due to porosity, CNT yarns impregnated with epoxy resin experience both mechanical and electrical structural changes. High twist in yarns bounds the fibers closer, restricting matrix ingress. Low twist yarns are highly permeable increasing both the strength after curing and the electrical resistance due to tunneling. Also, when the packing density of CNTs bundles in the yarn is high, electron mobility increases, leading to an increase in the conductivity of the CNT yarn. In the presence of a matrix, the gauge factors are higher for the CNT yarn. There is also increased linearity for CNT yarns coated with a polymer when compared to the uncoated one for the same strain level.
9. By subjecting a CNT yarn embedded into a polymer medium to four-point bending and uniaxial tension, the piezoresistive response of the constrained CNT yarns was determined under tension and compression. The relative resistance change of both the constrained and unconstrained CNT yarn increases monotonically with the strain. However, the piezoresistive response of the constrained CNT yarns is much more sensitive than that of the unconstrained CNT yarns. This difference between them may be explained by the lack of the effective slippage, fiber unraveling and subsequently, Poisson's effect, of the CNT yarn when constrained by the polymer. The composite samples tested under bending showed a higher gauge factor than under uniaxial tension. Higher sensitivity was observed for the samples tested at higher strain rates with gauge factors increasing with increasing strain levels. The negative piezoresistivity experienced by a free CNT yarn under low strain rate conditions was not encountered at similar strain rates for the constrained CNT yarn. Therefore, a foregone conclusion is that slippage plays a deeper role in the resistance decrease of CNT yarns upon loading at low strain rates.
10. The piezoresistive response of the constrained CNT yarns under compression was observed to exhibit a quasi-parabolic response. Like in the tensile tests, the relative change in resistance decreases slightly at first reaching a local minimum and tends to increase later. The hypotheses that were used to explain the phenomena of the CNT yarn under tension could also be applied in the case of the constrained CNT yarns under compression. Increased fiber density means charge carriers becomes closer and

the resistance decreases. The relative change in resistance also decreases. Therefore, a higher gauge factor is obtained under tension than under compression.

11. The ability of integrated carbon nanotube yarns to simply detect and even warn of an impending delamination and other damage in laminated composite materials including providing its exact location and extent had been proved. This last year, integrated fiber optics were used to validate the findings. In addition, x-ray microtomography was also used to validate the results using images after the tests. Both techniques confirm the results obtained with the integrated CNT yarn sensors.
12. CNT yarn-based strain sensor has outperformed the other macroscopic CNT structures in terms of sensitivity required for wearable electronics. The first foil strain gauge prototypes were built and calibrated exhibiting GF values above 30. The actualization of robust, flexible and stretchable CNT strain sensors still needs thorough research efforts. The potential of CNT yarns strain sensors is even more promising considering the competitive advantages CNTs have over current alternatives.